

Calculated Electronic Transitions in Sulfuric Acid and Implications for Its Photodissociation in the Atmosphere

Joseph R. Lane[†] and Henrik G. Kjaergaard^{*,†,‡}

Department of Chemistry, University of Otago, P.O. Box 56, Dunedin 9054, New Zealand, and The Lundbeck Foundation Center for Theoretical Chemistry, Department of Chemistry, Aarhus University, DK-8000 Aarhus C, Denmark

Received: November 13, 2007; Revised Manuscript Received: February 26, 2008

We have calculated electronic transitions for sulfuric acid in the ultraviolet region using a hierarchy of coupled cluster response functions and correlation consistent basis sets. Our calculations indicate that the lowest energy singlet transition occurs at 8.42 eV with an oscillator strength of 0.01. The lowest energy triplet state occurs at 8.24 eV. Thus, the cross section of sulfuric acid in the actinic region is likely to be very small and smaller than the upper limit put on this cross section by previous experimental investigations. We estimate the cross section of sulfuric acid in the atmospherically relevant Lyman- α region (~ 10.2 eV) to be $\sim 6 \times 10^{-17}$ cm² molecule⁻¹, a value approximately 30 times larger than the speculative value used in previous atmospheric simulations. We have calculated the J values for photodissociation of sulfuric acid with absorption of visible, UV, and Lyman- α radiation, at altitudes between 30 and 100 km. We find that the dominant photodissociation mechanism of sulfuric acid below 70 km is absorption in the visible region by OH stretching overtone transitions, whereas above 70 km, absorption of Lyman- α radiation by high energy Rydberg excited states is the favored mechanism. The low lying electronic transitions of sulfuric acid in the UV region do not contribute significantly to its dissociation at any altitude.

Introduction

The concentration and distribution of sulfur compounds in the atmosphere have been of increasing interest because of the important role they play in the formation of stratospheric aerosol.^{1–5} Sulfuric acid (H₂SO₄) is the dominant form of atmospheric sulfur in the stratosphere, with lesser amounts of sulfur trioxide (SO₃) and sulfur dioxide (SO₂).⁶ Sulfuric acid is very hygroscopic and so readily forms hydrated aerosol in the lower stratosphere. At higher altitudes, where the concentration of water is lower, H₂SO₄ exists primarily in the gas phase. At altitudes between 15 and 30 km, a highly dispersed layer of sulfate aerosol (Junge layer) exists, which influences Earth's climate through both radiative and chemical effects.³

Anomalous enhancement of the Junge layer in the polar springtime is thought to be a result of H₂SO₄ photodissociation.^{3,7,8} This photodissociation process was initially assumed to occur via absorption of an ultraviolet (UV) photon to a dissociative electronically excited state. However, several attempts to measure the electronic absorption spectrum of H₂SO₄ in the laboratory have been unable to identify any absorption up to 140 nm (8.6 eV).^{6,9} These experimental efforts have led to the following upper limits for the cross section of H₂SO₄, 10⁻²¹ cm² molecule⁻¹ in the region 330–195 nm, 10⁻¹⁹ cm² molecule⁻¹ in the region 195–160 nm, and 10⁻¹⁸ cm² molecule⁻¹ in the region 160–140 nm.

The electronic absorption spectrum of H₂SO₄ has been calculated previously with the CIS, TDDFT, CASSCF, and MRCISD methods.^{9–11} Of these methods, only the MRCISD calculations can be considered reliable for the accurate prediction

of electronic transitions. With the MRCISD/AVTZ method, the lowest energy electronic transition in H₂SO₄ was predicted to occur at 144 nm (8.61 eV), resulting in a very small calculated cross section in the actinic region.¹¹ This result is in agreement with the experimental investigations of Burkholder et al.⁶ and Hintze et al.⁹ Given that very few photons with wavelengths shorter than 179 nm penetrate the stratosphere,¹² UV photodissociation of H₂SO₄ is unlikely to be significant at lower altitudes.³

On the basis of early work by Crim,^{13,14} Vaida et al. proposed that excitation of OH-stretching overtone transitions in H₂SO₄ with visible photons could provide sufficient energy for photodissociation.³ The energy required for dissociation of H₂SO₄ \rightarrow H₂O + SO₃ has been calculated to be in the range 32–40 kcal mol⁻¹,^{15,16} hence, excitation of an OH-stretching transition with $\Delta\nu \geq 4$ (13 490 cm⁻¹ or 39 kcal mol⁻¹) should provide sufficient energy for dissociation.³ The importance of overtone induced photodissociation reaction mechanisms have been shown in both laboratory and field measurements for atmospheric radical production from, for example, hydrogen peroxide,^{17–19} nitric acid,^{20,21} peroxyxynitrous acid,^{21–25} and hydroxymethyl hydroperoxide.²⁶ However, experimental confirmation of the OH-stretching overtone induced photodissociation of H₂SO₄ has remained elusive. We have recently suggested that the inherent difficulties in observing H₂SO₄ photodissociation could be circumvented by monitoring the dissociation of a related compound, fluorosulfonic acid.²⁷

Atmospheric modeling studies have shown that the cross section of the very weak OH-stretching overtone transitions^{9,28} of H₂SO₄ are adequate to account for the inferred photodissociation rate, as a source of polar stratospheric sulfate aerosol.^{3,4} Furthermore, sufficient H₂SO₄ vapor survives this weak photodissociation mechanism to produce significant sulfate aerosol in the mesosphere.⁵ While the flux of visible photons is essentially constant with altitude, the flux of UV and in particular

* To whom correspondence should be addressed. E-mail: henrik@alkali.otago.ac.nz. Fax: 64-3-479-7906. Phone: 64-3-479-5378.

[†] University of Otago.

[‡] Aarhus University.

Lyman- α (121.6 nm) photons increases with altitude. In the mesosphere and above, the flux of Lyman- α photons is appreciable, and hence molecules with a large cross section in the region of Lyman- α radiation can photodissociate via high energy electronic excited states.²⁹

In this work, we investigate both the lowest lying electronic states of H_2SO_4 and the states in the region of Lyman- α radiation. We use a twin hierarchy of coupled cluster response functions in combination with augmented correlation consistent basis sets. This approach provides convergent results and hence an estimate of the accuracy, which is essential in the absence of experimental spectra.^{30,31} We simulate the electronic absorption spectrum of H_2SO_4 by convoluting the calculated electronic transitions with an empirical bandwidth and band shape determined from experimental spectra of SO_2 and SO_3 .^{9,32,33} We use the simulated cross sections to calculate the J values for photodissociation of H_2SO_4 with absorption of visible, UV, and Lyman- α radiation, at altitudes between 30 and 100 km. We compare these calculated J values to assess which of the competing photodissociation mechanisms is likely to dominate at a given altitude.

Theory and Calculations

We have calculated the vertical excitation energies and oscillator strengths of H_2SO_4 using coupled cluster response theory. A hierarchy of coupled cluster response methods were used, including coupled cluster singles (CCS), second order approximate coupled cluster singles and doubles (CC2), coupled cluster singles and doubles (CCSD), and third order approximate coupled cluster singles, doubles, and triples (CC3). For excited states dominated by a single excitation relative to the reference state, the coupled cluster methods are considered to be among the most accurate currently available.³⁴ To verify that the excited states are dominated by single excitation vectors, we compare the T1% diagnostic (the percentage of single excitations) for the excited states of H_2SO_4 . We have also investigated the excited states of H_2SO_4 with the less computationally demanding EOM-CCSD method. EOM-CCSD is closely related to CCSD linear response, with the same size-extensive excitation energies obtained with the two methods.³⁵

We have used the Dunning type correlation consistent basis sets supplemented with additional tight d basis functions on sulfur, aug-cc-pV(D+d)Z, aug-cc-pV(T+d)Z, and aug-cc-pV(Q+d)Z.³⁶ For brevity, we refer to these basis sets as AV(X+d)Z, where X is the cardinal number. The additional tight d functions have been shown to significantly improve the geometries and energies of sulfur-containing compounds and weakly bound complexes.^{37–39}

To ensure saturation of diffuse basis functions for some of the highly delocalized Rydberg excited states, we have also constructed a series of molecule-centered primitive basis functions, originating from the center of mass. These basis functions were generated according to the procedure by Kaufmann et al.⁴⁰ We have chosen a set of 3s3p3d functions with “semi-quantum numbers” from 2.0 to 3.0, in half-integral steps. The AV(X+d)Z basis sets augmented with this 3s3p3d set are denoted AV(X+d)Z+3. To test that our AV(X+d)Z+3 basis set is adequate, we have also constructed a much larger and more diffuse AV(D+d)+7 basis set, which includes a set of 7s7p7d molecule-centered functions with “semi-quantum numbers” from 2.0 to 5.0, in half-integral steps. Previously, basis sets of this type have been shown to adequately describe the $n = 3, 4, 5$ Rydberg states of s, p, d type in furan and pyrrole.^{30,31}

All coupled cluster calculations assume a frozen core (O:1s; S:1s,2s,2p). Coupled cluster response calculations were per-

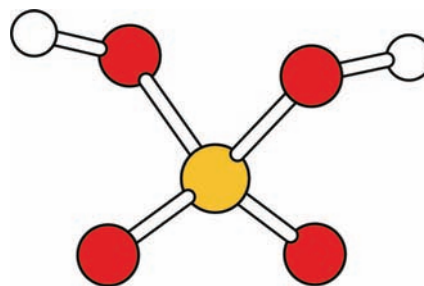


Figure 1. Experimental geometry of H_2SO_4 determined by microwave spectroscopy.⁴³

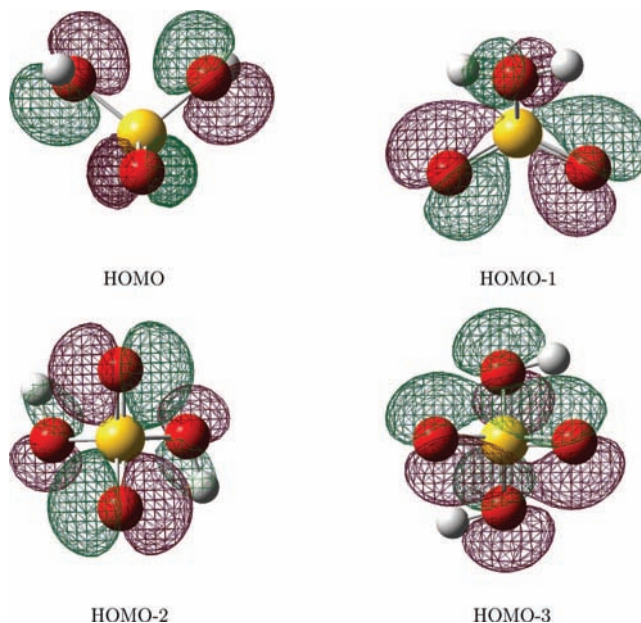


Figure 2. Selected Hartree-Fock molecular orbitals of H_2SO_4 .

formed using a local version of Dalton 2.0 at Aarhus University.⁴¹ EOM-CCSD calculations were performed with Molpro 2006.1.⁴²

Results and Discussion

The experimental geometry of H_2SO_4 as determined by microwave spectroscopy was used in all excited-state calculations and is shown in Figure 1.⁴³ The structure of H_2SO_4 has been investigated recently at the CCSD(T) level of theory, with the calculated geometry found to be in excellent agreement with the experimental geometry.^{39,44}

Sulfuric acid has a total of 22 valence molecular orbitals (MOs), of which 16 are occupied and 6 are unoccupied (virtual). The electronic configuration of H_2SO_4 in the 1A ground state is given by (*core*)¹⁸ $6a^25b^27a^26b^28a^27b^29a^28b^210a^29b^211a^210b^2-12a^211b^213a^212b^214a^013b^014b^015a^015b^016a^0$ where a and b are the symmetries of the MOs and the superscripts 0 and 2 are the number of electrons in each MO. In Figure 2, we present the four highest energy occupied Hartree-Fock molecular orbitals of H_2SO_4 , from which the excitations primarily occur.

Method Convergence. In Figure 3, we present the vertical excitation energies for the lowest energy excited states of H_2SO_4 calculated with the coupled cluster hierarchy and the AV(D+d)Z+3 basis set. In general, we see good convergence in the calculated vertical excitation energies with the hierarchy of coupled cluster methods. The CCS method overestimates the vertical excitation energies of H_2SO_4 by 1–2 eV. The inclusion of approximate double excitations with the CC2 method is a significant

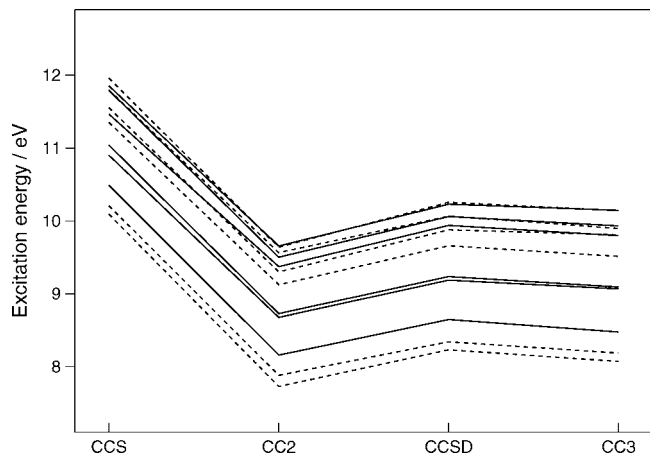


Figure 3. Vertical excitation energies for the lowest electronic excited states of H_2SO_4 calculated with different coupled cluster models using the AV(D+d)Z+3 basis set. Solid lines are 1A symmetry; dotted lines are 1B symmetry.

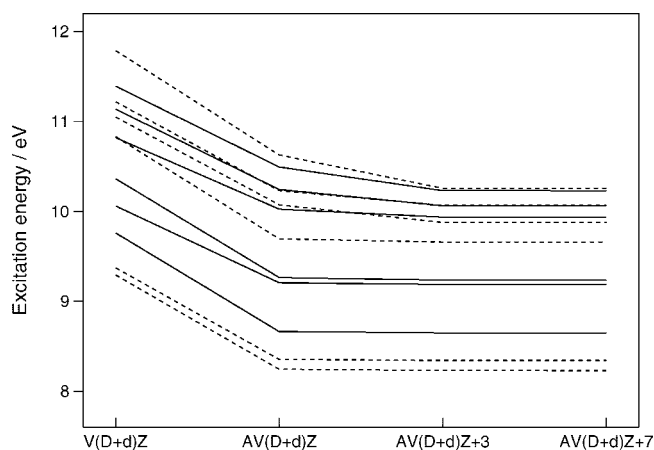


Figure 4. CCSD vertical excitation energies for the lowest electronic excited states of H_2SO_4 calculated with different numbers of diffuse basis functions. Solid lines are 1A symmetry; dashed lines are 1B symmetry.

improvement over CCS, with vertical excitation energies underestimated by several tenths of an electronvolt. Vertical excitation energies calculated with the CCSD method are 0.07–0.17 eV higher in energy than those calculated with CC3. At the CCSD level of theory, the average T1% of the excited states is 94%, and at the CC3 level of theory, the T1% drops to 91%. The relatively small variation between the CCSD and CC3 vertical excitation energies and the CCSD and CC3 T1% indicates that the excited states of H_2SO_4 are well-described by the CCSD level of theory.^{45–47}

Basis Set Convergence. In Figure 4, we present the CCSD calculated vertical excitation energies for the lowest energy excited states of H_2SO_4 calculated using the V(D+d)Z basis set augmented with various diffuse basis functions. We see good convergence of the vertical excitation energies as we increase the number of diffuse functions. Vertical excitations calculated with the V(D+d)Z basis are overestimated by as much as 1.5 eV, highlighting the importance of diffuse basis functions for an adequate description of excited states. The addition of a single shell of diffuse basis functions [AV(D+d)Z] significantly improves the calculated vertical excitation energies, although the higher energy states are still overestimated by several tenths of an electronvolt. These higher energy states, which are likely to have significant Rydberg character, require larger more spatially diffuse basis sets. For example, the fourth and sixth

TABLE 1: CCSD Vertical Excitation Energies (in Electronvolts) and Oscillator Strengths for H_2SO_4

state	AV(D+d)Z+3		AV(T+d)Z+3		AV(Q+d)Z+3 ^a
	<i>E</i>	<i>f</i>	<i>E</i>	<i>f</i>	<i>E</i>
1A	8.65	0.0018	8.83	0.0017	8.91
1A	9.19	0.0072	9.40	0.0061	9.49
1A	9.24	0.0071	9.44	0.0077	9.53
1A	9.94	0.0282	10.12	0.0445	10.20
1A	10.06	0.0633	10.21	0.0476	10.31
1A	10.23	1×10^{-5}	10.38	0.0003	10.44
1B	8.23	0.0097	8.42	0.0104	8.50
1B	9.34	0.0014	8.56	0.0019	8.65
1B	9.66	0.0232	9.86	0.0214	9.94
1B	9.88	0.0033	10.10	0.0048	10.19
1B	10.06	0.1193	10.27	0.1241	10.35
1B	10.26	0.0062	10.50	0.0039	10.59

^a Calculated with the EOM-CCSD method.

1B states have increased $\langle z^2 \rangle$ components of the second moment of charge distribution (given in Supporting Information) and are therefore more diffuse than the other states.

A common approach to constructing even more diffuse basis sets is to augment with two or more shells of diffuse basis functions, that is, d-aug-cc-pV(D+d)Z, t-aug-cc-pV(D+d)Z, and so forth. While this approach is very thorough, a great number of diffuse basis functions is required to achieve a converged solution. An alternative approach is to place a small number of very diffuse molecule centered basis functions at the center of mass or center of charge.⁴⁰ The AV(D+d)Z+3 basis set includes 27 [$3 \times (1 + 3 + 5)$] highly diffuse basis functions that have the correct nodal structure for describing Rydberg excited states.⁴⁰ For the lower energy states, there is little variation in the vertical excitation energies calculated with the AV(D+d)Z and AV(D+d)Z+3 basis sets. However, for some of the higher energy states, for example, the sixth 1A state and sixth 1B state, the effect of the highly diffuse basis functions is significant. Vertical excitation energies and oscillator strengths calculated with the AV(D+d)Z+3 basis set are in excellent agreement with those calculated with the much larger AV(D+d)Z+7 basis set, indicating that our system is saturated with diffuse basis functions with the AV(D+d)Z+3 basis set.

In Table 1, we investigate the change in the calculated vertical excitation energies and oscillator strengths that results from increasing the cardinal number of the basis set. We present the CCSD/AV(D+d)Z+3 and CCSD/AV(T+d)Z+3 results as well as the EOM-CCSD/AV(Q+d)Z vertical excitation energies. The calculated vertical excitation energies increase and converge as the size of the basis set increases. Vertical excitation energies calculated with the AV(T+d)Z+3 basis set are 0.18–0.25 eV higher than the AV(D+d)Z+3 results, and the EOM-CCSD/AV(Q+d)Z+3 energies are 0.06–0.09 eV higher than the CCSD/AV(T+d)Z+3 results. This variation in vertical excitation energies with the cardinal number of the basis set is similar to previous calculations on benzene, furan, and pyrrole and is an indication that in fact all of the states of H_2SO_4 considered have significant Rydberg character.^{30,31,48} For valence transitions, the effect of increasing the cardinal number of the basis set is expected to be much smaller. With the exception of the sixth 1A state and sixth 1B state, the oscillator strengths calculated with the CCSD/AV(D+d)Z+3 and CCSD/AV(T+d)Z+3 methods agree to within 40%.

Triplet Transitions. In Table 2, we present the CCSD calculated vertical excitation energies for the lowest lying triplet excited states of H_2SO_4 . We are unable to calculate the oscillator strengths for these spin forbidden transitions; however, spin

TABLE 2: CCSD Vertical Excitation Energies (in Electronvolts) for the Lowest Triplet Electronic States H₂SO₄

	AV(D+d)Z+3	AV(T+d)Z+3
³ A	8.46	8.64
³ A	8.91	9.13
³ A	9.13	9.33
³ A	9.65	9.80
³ A	9.91	10.07
³ A	10.12	10.27
³ B	8.04	8.24
³ B	8.09	8.30
³ B	9.31	9.48
³ B	9.63	9.81
³ B	9.73	9.92
³ B	10.05	10.18

forbidden transitions are inherently very weak with an oscillator strength typically of the order of 10^{-5} or less.⁴⁹ The vertical excitation energies calculated with the AV(D+d)Z+3 basis set are 0.13–0.21 eV less than those calculated with the AV(T+d)Z+3 basis set. This variation with basis set is similar to that observed for the singlet transitions of H₂SO₄. The lowest energy triplet state calculated with the AV(T+d)Z+3 basis set has a vertical excitation energy of 8.24 eV, which is only slightly lower than the lowest energy singlet state of H₂SO₄ (8.42 eV) calculated with the equivalent method. It is therefore unlikely that absorption by a triplet state will significantly contribute to the cross section of H₂SO₄.

Uncertainty Estimate. No electronic absorption features of H₂SO₄ have been observed in the visible and UV regions,^{6,9} so we are unable to assess the accuracy of our calculated electronic transitions by a direct comparison to experiment. However, the theoretical twin hierarchical approach provides convergent results and hence can be used to estimate the accuracy of our calculations. In this section, we estimate the accuracy of the CCSD/AV(T+d)Z+3 vertical excitation energies and oscillator strengths.

Vertical excitation energies calculated with the CCSD method were found to be 0.07–0.17 eV higher in energy than vertical excitation energies calculated with the CC3 method. Because of the convergent nature of the CC hierarchy, CCSD vertical excitation energies can be considered upper limits of a complete solution while the CC3 vertical excitation energies can be considered lower limits of a complete solution. Hence, we estimate that the effect of extending the CCSD model to include triple and higher order excitations will be an ~ 0.1 eV reduction in the calculated vertical excitation energies.

The AV(T+d)Z+3 basis set was found to include an appropriate number of diffuse basis functions to adequately describe the excited states considered in this investigation. Vertical excitation energies calculated with the EOM-CCSD/AV(Q+d)Z+3 method were found to be 0.06–0.09 eV greater than vertical excitation energies calculated with the CCSD/AV(T+d)Z+3 method. The systematic structure of the correlation consistent basis sets means that vertical excitation energies calculated with the AV(Q+d)Z+3 basis set will be a few hundredths of an electronvolt lower than vertical excitation energies calculated at the complete basis set limit. Hence, we estimate that the effect of extending the AV(T+d)Z+3 basis set to the complete basis set limit will increase the calculated vertical excitation energies by ~ 0.1 eV.

The effect of extending the CCSD/AV(T+d)Z+3 calculations of vertical excitation energies to include triple and higher order excitations and the effect of extending to the complete basis

set limit are likely to almost cancel. Thus, it seems that, because of a fortuitous cancellation of errors, our CCSD/AV(T+d)Z+3 vertical excitation energies are expected to be within ~ 0.1 eV of the theoretical limit.

The convergence of calculated oscillator strengths with the CC method and basis set is not as uniform as that for calculated vertical excitation energies. The calculation of CC3 oscillator strengths for H₂SO₄ is very computationally demanding, and we have only calculated oscillator strengths for the two lowest energy ¹A states and ¹B states with the CC3/AV(D+d)Z method. For these four lowest energy states, we find the CCSD/AV(D+d)Z oscillator strengths to be within $\sim 60\%$ of the CC3/AV(D+d)Z results (please see Supporting Information for more details). With the exception of the sixth ¹A state and sixth ¹B state, the oscillator strengths calculated with the CCSD/AV(D+d)Z+3 and CCSD/AV(T+d)Z+3 methods agree to within 40%. For these reasons, we estimate that our CCSD/AV(T+d)Z+3 calculated oscillator strengths are within a factor of 2 of the theoretical limit.

As a final check, we also estimate the error in our CCSD/AV(T+d)Z+3 vertical excitation energies and oscillator strengths for H₂SO₄ by comparing with calculations for sulfur dioxide (SO₂), for which high quality experimental spectra including absolute intensities are available.³² Vertical excitation energies for SO₂ calculated with the CCSD/AV(T+d)Z+3 method were found to be ~ 0.3 eV higher than the measured band maxima of the predominantly valence transitions and ~ 0.1 eV higher than the measured band maxima of the predominantly Rydberg transitions. With the exception of the weak \tilde{A} band in SO₂, oscillator strengths of the predominantly valence transitions calculated with the CCSD/AV(T+d)Z+3 method were found to be within a factor of 2 of the experimental results. For the higher energy predominantly Rydberg transitions, the calculated oscillator strengths were found to be within 20% of the experimental results. The greater discrepancies observed between the calculated vertical excitation energies and the experimental band maxima of the predominantly valence transitions in SO₂ are likely due to the more significant variation between the ground-state and excited-state geometries of these lower energy states. Nonetheless, the agreement between the ab initio calculated electronic transitions and the experimental spectra for SO₂ indicates that our calculated results for H₂SO₄ (at the same level of theory) are likely to be of an accuracy useful for atmospheric modeling.

Cross Section. In Figure 5, we simulate the cross section of H₂SO₄ by convoluting the CCSD/AV(T+d)Z+3 calculated vertical excitation energies and oscillator strengths with a Gaussian band shape. We convolute the electronic transitions using two different bandwidths for the lower and higher energy transitions, respectively. The three lowest energy states of ¹A and ¹B symmetry are convoluted with a half-width at half-maximum (HWHM) of 0.47 eV (3800 cm⁻¹). This bandwidth is approximately the HWHM of the lowest lying valence electronic transitions in sulfur dioxide and sulfur trioxide.^{9,32,33} The fourth, fifth, and sixth states of ¹A and ¹B symmetry are convoluted using a HWHM of 0.15 eV (1200 cm⁻¹). This much narrower bandwidth is approximately the HWHM of the Rydberg transitions in sulfur dioxide around 10 eV.³²

In general, our simulated spectrum supports the experimental upper limits for the cross section of H₂SO₄ in the visible and UV regions determined by Burkholder et al.⁶ and Hintze et al. and shown in Figure 5 as horizontal lines.⁹ The maximum calculated cross section of H₂SO₄ in the UV region is $\sim 1.6 \times 10^{-18}$ cm² molecule⁻¹, which is slightly larger than the

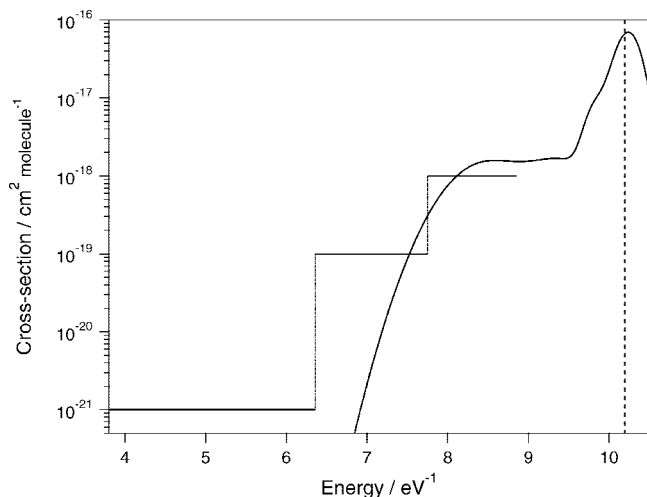


Figure 5. Cross section of H_2SO_4 simulated from CCSD/AV(T+d)Z+3 calculated electronic transitions. Each electronic transition has been convoluted with a Gaussian with a HWHM of 0.47 eV for the transitions below 9.5 and 0.15 eV for the higher energy transitions. Experimental upper limits have been indicated with connected horizontal lines. The Lyman- α energy is indicated by a vertical dashed line.

experimentally determined upper limit of $10^{-18} \text{ cm}^2 \text{ molecule}^{-1}$. However, uncertainty in the bandwidth, band shape, and oscillator strengths of the calculated electronic transitions and uncertainty in the experimental upper limits probably means that our calculated cross section is consistent with the experimental upper limit. This result is also in agreement with the previous MRCISD/AVTZ calculations of Robinson et al.¹¹

Our simulated spectrum indicates a large cross section of $6.6 \times 10^{-17} \text{ cm}^2 \text{ molecule}^{-1}$ for H_2SO_4 in the region of Lyman- α radiation ($\sim 10.2 \text{ eV}$). The accuracy of this cross section depends on several variables including the absolute vertical excitation energies, the calculated oscillator strengths, and the bandwidth used for convolution. We estimate that the calculated vertical excitation energies for H_2SO_4 in the Lyman- α region are within $\sim 0.1 \text{ eV}$ of the actual values. If we red- or blueshift the calculated vertical excitation energies by 0.1 eV, the cross section of H_2SO_4 becomes $6.4 \times 10^{-16} \text{ cm}^2 \text{ molecule}^{-1}$ and $4.3 \times 10^{-16} \text{ cm}^2 \text{ molecule}^{-1}$, respectively. We estimate the error in our calculated oscillator strengths to be within a factor of 2; hence, if we double or half the calculated oscillator strengths, the cross section of H_2SO_4 becomes $1.6 \times 10^{-16} \text{ cm}^2 \text{ molecule}^{-1}$ and $2.4 \times 10^{-17} \text{ cm}^2 \text{ molecule}^{-1}$, respectively. The bandwidth of the lower energy transitions does not impact the cross section at Lyman- α . If we double or half the 1200 cm^{-1} HWHM of the high energy transitions used to convolute the spectra, the cross section of H_2SO_4 becomes $3.9 \times 10^{-17} \text{ cm}^2 \text{ molecule}^{-1}$ and $8.6 \times 10^{-17} \text{ cm}^2 \text{ molecule}^{-1}$, respectively. In summary, we estimate that the cross section of H_2SO_4 in the Lyman- α region to be in the range $2 \times 10^{-17} \text{ cm}^2 \text{ molecule}^{-1}$ to $2 \times 10^{-16} \text{ cm}^2 \text{ molecule}^{-1}$. Our calculated cross section of H_2SO_4 in the Lyman- α region is 10–100 times greater than the previous estimate used in early atmospheric modeling of $2 \times 10^{-18} \text{ cm}^2 \text{ molecule}^{-1}$.^{6,50,51}

Atmospheric J Values. The photodissociation rate constant (J) for H_2SO_4 can be calculated using the following equation

$$J = \int I(\nu)\Phi(\nu)\sigma(\nu)d\nu \quad (1)$$

where $I(\nu)$ is the frequency dependent solar flux, $\Phi(\nu)$ is the quantum yield, and $\sigma(\nu)$ is the cross section.¹²

In Figure 6, we present the cross section for H_2SO_4 and the solar flux at 80 km in the visible, UV, and Lyman- α regions.

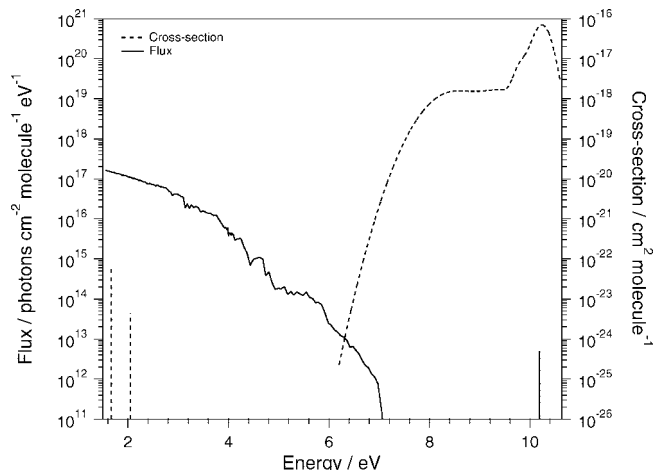


Figure 6. Simulated absorption cross section of H_2SO_4 and the solar flux at 80 km. See text for details.

The cross section in the visible region around 2 eV corresponds to absorption via the $\Delta\nu_{\text{OH}} = 4$ and 5 vibrational transitions.^{3,28} The cross section in the UV region ($\sim 6 \text{ eV}$) corresponds to the absorption tail of the calculated low energy electronic transitions whereas the cross section in the Lyman- α region ($\sim 10 \text{ eV}$) corresponds to absorption of the high energy electronic transitions. We use the TUV radiation model to calculate the solar flux from 120 to 800 nm (1.55 to 10.3 eV).⁵² The calculated flux is averaged over a 24 h period, for 26° N to 32° N , from April to May. This is similar to the conditions used by Mills et al. for modeling the SO_2 profile as a product of sulfuric acid photodissociation.⁴ As seen in Figure 6, the H_2SO_4 absorption cross section in the visible region is limited to very small narrow bands while the flux of solar photons is high. Conversely, in the region of Lyman- α radiation, the cross section of H_2SO_4 is very large while the flux of solar photons is small and limited to a narrow region. In the UV region, both the cross section of H_2SO_4 and the flux of solar photons are small; hence, this photodissociation mechanism is unlikely to contribute significantly in the atmosphere. The flux of photons in the visible region is more or less constant at all altitudes whereas the flux of photons in the Lyman- α region is strongly dependent on altitude.¹² It follows that the dominant mechanism for H_2SO_4 photodissociation in the atmosphere is likely to depend on the altitude of reaction.

In Figure 7, we present the J values for photodissociation of H_2SO_4 calculated at various altitudes. The visible J values correspond to the OH-stretching overtone induced photodissociation mechanism proposed by Vaida et al.,³ with experimental integrated cross sections for $\Delta\nu_{\text{OH}} = 4$ and 5 transitions from Feierabend et al.²⁸ and quantum yield estimates from Miller et al.⁵³ For comparison, we also show the visible $\text{QY} = 1$ J values, which use the same OH-stretching overtone induced photodissociation mechanism but assume a quantum yield of unity at all altitudes. For the UV and Lyman- α J values, a quantum yield of unity is assumed for all altitudes. The UV J values correspond to photodissociation in the UV region (160–220 nm, 5.6–7.8 eV), using the cross section in the tail of the simulated spectra (Figure 5) obtained with the calculated CCSD/AV(T+d)Z+3 lower energy electronic transitions. The Lyman- α J values correspond to photodissociation by Lyman- α photons, using the cross section of the simulated spectra (Figure 5) obtained with the calculated CCSD/AV(T+d)Z+3 electronic transitions in the region of Lyman- α radiation.

At altitudes below 60 km, the OH-stretching overtone induced photodissociation mechanism is likely to dominate. While the

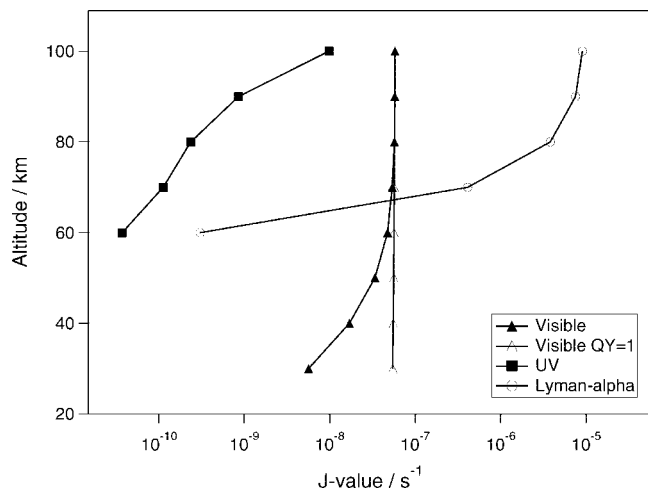


Figure 7. J values for the photodissociation mechanisms of H_2SO_4 at different altitudes. See text for details.

integrated cross section of these overtone transitions is very small, there is a large flux, and hence, the J value is several orders of magnitude greater than that for the UV and Lyman- α photodissociation mechanisms. The Earth's atmosphere is essentially transparent in the visible region, which leads to an almost constant flux in the visible region at all altitudes. This effect can be seen from the Visible QY=1 J values, which are almost constant at all altitudes. The quantum yield of a photodissociation reaction is essentially determined by the relative rate of collisional deactivation and the rate of reaction.⁵³ At lower altitudes, the number density of Earth's atmosphere is greater than at higher altitudes, which leads to a higher rate of collisional deactivation and hence a lower quantum yield. This nonunity quantum yield reduces the J value of the OH-stretching overtone photodissociation mechanism at altitudes below 80 km.

The flux of photons in the UV region (including Lyman- α radiation) is dependent on altitude, with molecular oxygen and nitrogen absorbing strongly in this region. From 60 km to 100 km, the flux and hence the J value for the UV photodissociation mechanism increases 2 orders of magnitude. However, the small cross section of H_2SO_4 in this UV region means that, even at 100 km, the J value of the UV photodissociation mechanism is still an order of magnitude less than the OH-stretching overtone photodissociation mechanism. At 80 km and above, the flux of Lyman- α radiation is 5 orders of magnitude less than the flux in the visible region. Nevertheless, the cross section of H_2SO_4 in the region of Lyman- α radiation is 7 orders of magnitude greater than the cross section of the $\Delta\nu_{\text{OH}} = 4$ overtone transition. Thus at altitudes above 80 km, this large cross section results in a J value for Lyman- α photodissociation that is more than 2 orders of magnitude greater than the J value for the OH-stretching overtone photodissociation mechanism. Even at the lower limit of our simulated Lyman- α cross section, the J value for Lyman- α photodissociation at 80 km is approximately 2 orders of magnitude greater than the J value for the OH-stretching overtone photodissociation mechanism.

In summary, we find that at altitudes below 60 km, photodissociation of H_2SO_4 is likely to occur via the OH-stretching overtone induced photodissociation mechanism. Our present J values for this photodissociation mechanism are consistent with the previous work of Vaida et al.³ At 70 km, the J value for Lyman- α photodissociation is approximately equal to the J value for the OH-stretching overtone photodissociation mechanism.

At altitudes above 80 km, photodissociation of H_2SO_4 is likely to occur via the Lyman- α photodissociation mechanism.

Conclusions

We have calculated electronic transitions for H_2SO_4 up to 10.5 eV. We have used a hierarchy of coupled cluster response functions and correlation consistent basis sets to assess the accuracy of our results. We find the CCSD/AV(T+d)Z+3 method to be reasonably well converged and expect our calculated vertical excitation energies and oscillator strengths for H_2SO_4 to be close to the theoretical limit. For SO_2 , we find results obtained with the CCSD/AV(T+d)Z+3 method to be in good agreement with the available experimental spectra. We find the lowest energy singlet state of H_2SO_4 to have a vertical excitation energy of 8.42 eV and an oscillator strength of 0.01. The lowest energy triplet state has a vertical excitation energy of 8.24 eV and is unlikely to contribute significantly to the cross section of H_2SO_4 in the actinic region. Our present calculations support the experimental upper limits for the cross section of H_2SO_4 in the actinic region. We estimate the cross section of H_2SO_4 in the Lyman- α region to be $\sim 6 \times 10^{-17} \text{ cm}^2 \text{ molecule}^{-1}$. This cross section value is more than 1 order or magnitude greater than the previous estimate used in atmospheric modeling studies. At altitudes below 70 km, we find that the photodissociation of H_2SO_4 is likely to proceed via absorption of high energy OH-stretching overtone transitions. At altitudes above 70 km, we find that the photodissociation of H_2SO_4 is likely to proceed via absorption of Lyman- α photons. The photodissociation of H_2SO_4 via absorption in the UV region is unlikely to contribute significantly in the atmosphere.

Acknowledgment. We thank Filip Pawlowski, Poul Jørgensen, Paul Wennberg, and Veronica Vaida for helpful discussions. J.R.L. is grateful to the Foundation for Research, Science and Technology for a Bright Futures scholarship. We acknowledge the Centre for Scientific Computing in Aarhus (CSC-AA) and the Lasers and Applications Research Theme at the University of Otago for use of their computer facilities. We acknowledge the Marsden Fund administered by the Royal Society of New Zealand, the Lundbeck Foundation, and the Research Foundation at Aarhus University for financial support.

Supporting Information Available: The calculated vertical excitation energies in tabular format for Figures 3 and 4; CCS, CC2, CCSD, and CC3 oscillator strengths calculated with the AV(D+d)Z basis set; CCSD oscillator strengths calculated with the V(D+d)Z, AV(D+d)Z, AV(D+d)Z+3, and AV(D+d)Z+7 basis sets; CCSD/AV(T+d)Z+3 vertical excitation energies, oscillator strengths, and one-electron properties. This material is available free of charge via the Internet at <http://pubs.acs.org>.

References and Notes

- (1) Charlson, R. J.; Anderson, T. L.; McDuff, R. E. *Earth System Science Academic Press*: New York, 2000.
- (2) Warneck, P. *Chemistry of the Natural Atmosphere*; Academic Press: San Diego, 2000; 2nd ed.
- (3) Vaida, V.; Kjaergaard, H. G.; Hintze, P. E.; Donaldson, D. J. *Science* **2003**, *299*, 1566.
- (4) Mills, M. J.; Toon, O. B.; Vaida, V.; Hintze, P. E.; Kjaergaard, H. G.; Schofield, D. P.; Robinson, T. W. *J. Geophys. Res. Atmos.* **2005**, *110*, D08201.
- (5) Mills, M. J.; Toon, O. B.; Thomas, G. E. *J. Geophys. Res.* **2005**, *110*, D24208.
- (6) Burkholder, J. B.; Mills, M. J.; McKeen, S. *Geophys. Res. Lett.* **2000**, *27*, 2493.
- (7) Rosen, J. M.; Hofmann, D. J. *J. Geophys. Res.* **1983**, *88*, 3725–3731.

- (8) Hofmann, D. J.; Rosen, J. M. *Geophys. Res. Lett.* **1985**, *12*, 13–16.
- (9) Hintze, P. E.; Kjaergaard, H. G.; Vaida, V.; Burkholder, J. B. *J. Phys. Chem. A* **2003**, *107*, 1112–1118.
- (10) Wrenn, S. J.; Butler, L. J.; Rowland, G. A.; Knox, C. J. H.; Phillips, L. F. *J. Photochem. Photobiol. A* **1999**, *129*, 101–104.
- (11) Robinson, T. W.; Schofield, D. P.; Kjaergaard, H. G. *J. Chem. Phys.* **2003**, *118*, 7226–7232.
- (12) Seinfeld, J. H.; Pandis, S. N. *Atmospheric Chemistry and Physics: From Air Pollution to Climate Change*; John Wiley & Sons: New York, 1998.
- (13) Crim, F. F. *Annu. Rev. Phys. Chem.* **1984**, *35*, 657–691.
- (14) Crim, F. F. *J. Phys. Chem.* **1996**, *100*, 12725–12734.
- (15) Morokuma, K.; Muguruma, C. *J. Am. Chem. Soc.* **1994**, *116*, 10316.
- (16) Larson, L. J.; Kuno, M.; Tao, F.-M. *J. Chem. Phys.* **2000**, *112*, 8830–8838.
- (17) Rizzo, T. R.; Hayden, C. C.; Crim, F. F. *Faraday Discuss. Chem. Soc.* **1983**, *75*, 223–237.
- (18) Scherer, N. F.; Zewail, A. H. *J. Chem. Phys.* **1987**, *87*, 97–114.
- (19) Ticich, T. M.; Likar, M. D.; Dubal, H. R.; Butler, L. J.; Crim, F. F. *J. Chem. Phys.* **1987**, *87*, 5820–5829.
- (20) Sinha, A.; Vander Wal, R. L.; Crim, F. F. *J. Chem. Phys.* **1990**, *92*, 401–410.
- (21) Donaldson, D. J.; Tuck, A. F.; Vaida, V. *Phys. Chem. Earth C* **2000**, *25*, 223–227.
- (22) Nizkorodov, S. A.; Wennberg, P. O. *J. Phys. Chem. A* **2002**, *106*, 855–859.
- (23) Roehl, C. M.; Nizkorodov, S. A.; Zhang, H.; Blake, G. A.; Wennberg, P. O. *J. Phys. Chem. A* **2002**, *106*, 3766–3772.
- (24) Konen, I. M.; Pollack, I. B.; Li, E. X. J.; Lester, M. I.; Varner, M. E.; Stanton, J. F. *J. Chem. Phys.* **2005**, *122*, 094320.
- (25) Fry, J. L.; Nizkorodov, S. A.; Okumura, M.; Roehl, C. M.; Francisco, J. S.; Wennberg, P. O. *J. Chem. Phys.* **2004**, *121*, 1432–1448.
- (26) Fry, J. L.; Matthews, J.; Lane, J. R.; Roehl, C. M.; Sinha, A.; Kjaergaard, H. G.; Wennberg, P. O. *J. Phys. Chem. A* **2006**, *110*, 7072–7079.
- (27) Lane, J. R.; Kjaergaard, H. G. *J. Phys. Chem. A* **2007**, *111*, 9707–9713.
- (28) Feierabend, K. J.; Havey, D. K.; Brown, S. S.; Vaida, V. *Chem. Phys. Lett.* **2006**, *420*, 438–442.
- (29) Brasseur, G. P.; Solomon, S. *Aeronomy of the middle atmosphere: chemistry and physics of the stratosphere and mesosphere*; Springer: Dordrecht, Netherlands, 2005.
- (30) Christiansen, O.; Jørgensen, P. *J. Am. Chem. Soc.* **1998**, *120*, 3423–3430.
- (31) Christiansen, O.; Gauss, J.; Stanton, J. F.; Jørgensen, P. *J. Chem. Phys.* **1999**, *111*, 525–537.
- (32) Feng, R.; Sakai, Y.; Zheng, Y.; Cooper, G.; Brion, C. E. *Chem. Phys.* **2000**, *260*, 29–43.
- (33) Burkholder, J. B.; McKeen, S. *Geophys. Res. Lett.* **1997**, *24*, 3201–3204.
- (34) Crawford, T. D.; Abrams, M. L.; Lane, J. R.; Schofield, D. P.; Kjaergaard, H. G. *J. Chem. Phys.* **2006**, *125*, 204302.
- (35) Helgaker, T.; Jørgensen, P.; Olsen, J. *Molecular Electronic Structure Theory*; John Wiley & Sons Ltd: Chichester, 2000.
- (36) Wilson, A. K.; Peterson, K. A.; Dunning, T. H. *J. Chem. Phys.* **2001**, *114*, 9244.
- (37) Wilson, A. K.; Dunning, T. H., jr. *J. Chem. Phys.* **2003**, *119*, 11712.
- (38) Garden, A. L.; Lane, J. R.; Kjaergaard, H. G. *J. Chem. Phys.* **2006**, *125*, 144317.
- (39) Lane, J. R.; Kjaergaard, H. G.; Plath, K. P.; Vaida, V. *J. Phys. Chem. A* **2007**, *111*, 5434–5440.
- (40) Kaufmann, K.; Baumeister, W.; Jungen, M. *J. Phys. B: At. Mol. Opt. Phys.* **1989**, *22*, 2223–2240.
- (41) Dalton, a molecular electronic structure program, release 2.0 (2005), see <http://www.kjemi.uio.no/software/dalton/dalton.html>. Angeli, C.; Bak, K. L.; Bakken, V.; Christiansen, O.; Cimiraglia, R.; Coriani, S.; Dahle, P.; Dalskov, E. F.; Enevoldsen, T.; Fernandez, B.; Hattig, C.; Hald, K.; Halkier, A.; Heiberg, H.; Helgaker, T.; Hettner, H.; Jensen, H. J. A.; Jonsson, D.; Jørgensen, P.; Kirpekar, S.; Klopper, W.; Kobayashi, R.; Koch, H.; Lutnaes, O. B.; Millelsen, K. V.; Norman, P.; Olsen, J.; Packer, M. J.; Pederson, T. B.; Rinkevicius, Z.; Rudberg, E.; Ruden, T. A.; Ruud, K.; Salek, P.; Sanchez de Meras, A.; Saue, T.; Sauer, S. P. A.; Schimmelpfennig, B.; Sylvester-Hvid, K. O.; Taylor, P. R.; Vahtras, O.; Wilson, D. J.; Agren, H. 2005.
- (42) Molpro, version 2006.1, a package of ab initio programs. Werner, H.-J.; Knowles, P. J.; Lindh, R.; Manby, F. R.; Schütz, M.; Celani, P.; Korona, T.; Rauhut, G.; Amos, R. D.; Bernhardsson, A.; Berning, A.; Cooper, D. L.; Deegan, M. J. O.; Dobbyn, A. J.; Eckert, F.; Hampel, C.; Hetzer, G.; Lloyd, A. W.; McNicholas, S. J.; Meyer, W.; Mura, M. E.; Nicklass, A.; Palmieri, P.; Pitzer, R.; Schumann, U.; Stoll, H.; Stone, A. J.; Tarroni, R.; Thorsteinsson, T. 2006.
- (43) Kuczukowski, R. L.; Suenram, R. D.; Lovas, F. J. *J. Am. Chem. Soc.* **1981**, *103*, 2561–2566.
- (44) Demaison, J.; Herman, M.; Lievin, J.; Rudolph, H. D. *J. Phys. Chem. A* **2007**, *111*, 2602–2609.
- (45) Öhrn, A.; Christiansen, O. *Phys. Chem. Chem. Phys.* **2001**, *3*, 730–740.
- (46) Hald, K.; Jørgensen, P.; Olsen, J.; Jaszunski, M. *J. Chem. Phys.* **2001**, *115*, 671–679.
- (47) Larsen, H.; Hald, K.; Olsen, J.; Jørgensen, P. *J. Chem. Phys.* **2001**, *115*, 3015–3020.
- (48) Christiansen, O.; Koch, H.; Halkier, A.; Jørgensen, P.; Helgaker, T.; Sanchez de Meras, A. *J. Chem. Phys.* **1996**, *105*, 6921–6939.
- (49) Atkins, P. W.; Friedman, R. S. *Molecular Quantum Mechanics*; Oxford University Press: Oxford, 1997; 3rd ed.
- (50) Rinsland, C. P.; Gunson, M. R.; Ko, M. K. W.; Weisenstein, D. W.; Zander, R.; Abrams, M. C.; Goldman, A.; Sze, N. D.; Yue, G. K. *Geophys. Res. Lett.* **1995**, *22*, 1109–1112.
- (51) Mills, M. J.; Toon, O. B.; Solomon, S. *Geophys. Res. Lett.* **1999**, *26*, 1133–1136.
- (52) Tropospheric ultraviolet-visible model (tuv). Madronich, S.; Flocke, S.; Zeng, J.; Petropavlovskikh, I.; Lee-Taylor, J. 2005.
- (53) Miller, Y.; Gerber, R. B.; Vaida, V. *Geophys. Res. Lett.* **2007**, *34*, L16820.